JOURNAL
OF THE
AMERICAN
CHEMICAL
SOCIETY

Expression of Binding Energy on an Antibody Reaction Coordinate

Herschel Wade and Thomas S. Scanlan*

Contribution from the Departments of Pharmaceutical Chemistry and Cellular and Molecular Pharmacology, University of California, San Francisco, California 94143-0446

Abstract: In this paper, we report the investigation of how the catalytic antibody 17E8 uses remote binding energy along the catalyzed hydrolytic reaction coordinate. With the use of alternative substrate analogues, we find that 17E8 can use free energy from binding interactions between the substrate side chain and antibody recognition pocket to equally stabilize the transition state and the Michaelis complex. In these cases, the interactions are not used to increase k_{cat}. We have also identified substrates for which the interactions are used to preferentially stabilize the transition state over the Michaelis complex. In these cases, the interactions are used to increase k_{cat}. Mechanistic studies support the idea that the differences in the substrates' kinetic activities results from differences in the expression of side-chain–pocket binding energy along the reaction coordinates. These results suggest that generating catalytic antibodies to transition-state analogues may be limited because the selective use of remote binding interactions cannot be programmed into transition-state analogues.

Enzymes use binding energy to place substrates in a precise position relative to catalytic groups in enzyme active sites. In addition, they are able to use binding energy gained from interactions with nonreacting portions of the substrate to stabilize the transition state of the reaction.[1-5] However, stabilization of the transition state (obtaining a large k_{cat}/K_M) is not the only requirement for efficient catalysis; it is also necessary to ensure rapid turnover (obtaining a large k_{cat}) by decreasing the free-energy difference between transition-state complex, $(E–S),$[‡] and the ground-state Michaelis complex, $(E–S)$.[6-8] Enzymes achieve

this by expressing binding energy selectively along the reaction coordinate. By using the free energy from binding interactions that either exclusively stabilize the $(E–S)^{‡}$ or that stabilize the $(E–S)^{‡}$ more than the $(E–S)$, enzymes achieve fast turnover and avoid the unproductive overstabilization of ground-state species.[1-4]

Structural and functional studies of catalytic antibodies have shown that the bulk of catalytic power results directly from the use of binding energy from interactions that are proximal to and remote from the catalytic center.[9-13] Indeed, the catalytic antibody 17E8 uses the energy from noncovalent interactions between the amino acid side chain of substrates and a side-chain recognition pocket, which are both removed from the

* To whom correspondence should be addressed: (phone) 415-476-3620; (fax) 415-476-0688; (e-mail) scanlan@cgl.ucsf.edu.

(1) Jencks, W. P. *Cold Spring Harbor Symp. Quant. Biol.* **1987**, *LII*, 65–73.

(2) Jencks, W. P. *Catalysis in Chemistry and Enzymology*; Dover Publications: Mineola, 1969.

(3) Fersht, A. R. *Proc. R. Soc. London Ser. B* **1974**, *187*, 397–407.

(4) Fersht, A. *Structure and Mechanism in Protein Science: A Guide to Enzyme Catalysis and Protein Folding*; W. H. Freeman and Company: New York, 1999.

(5) Pauling, L. *Chem. Eng. News* **1946**, *24*, 1375–1377.

(6) Avis, J. M.; Fersht, A. R. *Biochemistry* **1993**, *32*, 5321–5326.

(7) Whitty, A.; Fierke, C. A.; Jencks, W. P. *Biochemistry* **1995**, *34*, 11678–11689.

(8) Wells, T. N. C.; Fersht, A. R. *Biochemistry* **1986**, *25*, 1881–1886.

(9) Wade, H.; Scanlan, T. S. *J. Am. Chem. Soc.* **1999**, *121*, 1434–1443.

(10) Wade, H.; Scanlan, T. S. *Annu. Rev. Biophys. Biomol. Struct.* **1997**, *26*, 461–493.

(11) Ulrich, H. D.; Mundorff, E.; Santarsiero, B. D.; Driggers, E. M.; Stevens, R. C.; Schultz, P. G. *Nature (London)* **1997**, *389*, 271–275.
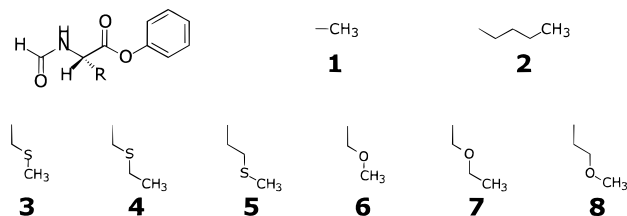
(12) Stewart, J. D.; Benkovic, S. J. *Nature (London)* **1995**, *375*, 388–391.

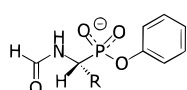(13) Benkovic, S. J. *Annu. Rev. Biochem.* **1992**, *61*, 29–54.

11936 *J. Am. Chem. Soc., Vol. 121, No. 51, 1999*

Wade and Scanlan
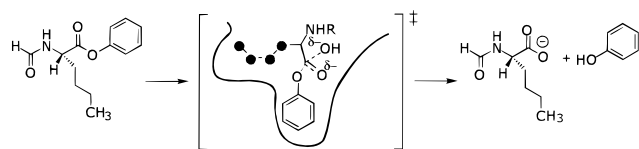
Figure 1. Hydrolytic reaction catalyzed by 17E8 and the transition state formed by hydroxide attack.

Figure 2. (A) Substrates used to study side-chain−pocket interactions. The *N*-formyl phenyl ester skeleton is shown above side-chains which are designated by R. (B) The *N*-formyl phenyl phosphonate skeleton of the transition-state analogues used in this study.

reactive center, to promote ester hydrolysis (Figure 1).[9,14] These interactions are analogous to those in natural enzymes such as proteases and tRNA synthetases that also use binding interactions between amino acid side chains and recognition pockets.[15−22]

In a previous study, we determined that the removal of the methylene groups from **2** to yield **1** (Figure 2) resulted in an increase in the free energy of the 17E8−substrate transition-state complex, indicating that 17E8 uses the side-chain−pocket interactions for overall transition-state stabilization (Table 1).[9,14] The removal of the interactions also resulted in a similar decrease in the stability of the Michaelis complex, indicating that 17E8 uses the side-chain−pocket interactions in a manner that has been termed *uniform binding*.[1−4] With *uniform binding*, the interactions are used to equally stabilize both the Michaelis and the transition-state complexes (Figure 3). Because the additional side-chain−pocket interactions are not used to decrease the free energy difference between the (IgG−S) and the (IgG−S)‡, which would result in an increased k_{cat} value, *uniform binding* can be viewed as a wasteful use of binding energy and a trait of a primitive catalyst.[2,3,23]

We have identified alternative substrates for which the binding energy between the amino acid side chain and recognition pocket is used to increase the catalytic turnover number (Figure 2). Here we show that the difference in the kinetic activity of these

(14) Wade, H.; Scanlan, T. S. *J. Am. Chem. Soc.* **1996**, *118*, 6510−6511.

(15) Bizzozero, S. A.; Baumann, W. K.; Dutler, H. *Eur. J. Biochem.* **1982**, *122*, 251−258.

(16) Bauer, C.-A.; Thompson, R. C.; Blout, E. R. *Biochemistry* **1976**, *15*, 1291−1296.

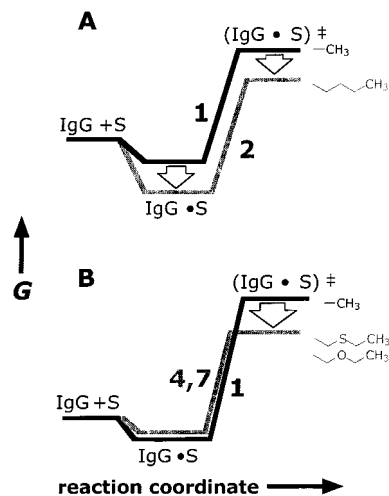(17) Thompson, R. C.; Blout, E. R. *Biochemistry* **1973**, *12*, 57−65.

(18) Thompson, R. C. *Biochemistry* **1974**, *13*, 5495−5501.

(19) Stroud, R. M. *Am. Sci.* **1974**, *231*, 74−88.

(20) Fersht, A. R.; Dingwall, C. *Biochemistry* **1979**, *18*, 1250−1255.

(21) Dorovska, V. N.; Varfolomeyev, S. D.; Kazanskaya, N. F.; Klyosov, A. A.; Martinek, K. *FEBS Lett.* **1972**, *23*, 122−124.

(22) Berezin, I. V.; Kazanskaya, N. F.; Klyosov, A. A.; Martinek, K. *FEBS Lett.* **1971**, *15*, 125−128.

Table 1. Steady-State Kinetic Analysis of Substrates[a,b]

	K_M (µM) [$\Delta\Delta G_s$ (kcal/mol)]	k_{cat} (s⁻¹) [$\Delta\Delta G^{\ddagger}$ (kcal/mol)]	k_{cat}/K_M (M·s)⁻¹ [$\Delta\Delta G_b$(kcal/mol)]
1	3400 ± 400 [0.0]	1.0 ± 0.1 [0.0]	290 ± 40 [0.0]
2	180 ± 30 [−1.7]	2.1 ± 0.1 [−0.4]	12000 ± 1400 [−2.1]
3	2600 ± 100 [−0.1]	18 ± 1 [−1.7]	7000 ± 100 [−1.8]
4	4000 ± 200 [+0.1]	43 ± 2 [−2.1]	11000 ± 700 [−2.0]
5	3400 ± 900 [0.0]	3.3 ± 0.5 [−0.7]	970 ± 300 [−0.6]
6	4600 ± 200 [+0.1]	12 ± 1 [−1.4]	2600 ± 100 [−1.2]
7	5000 ± 700 [+0.3]	27 ± 2 [−1.9]	5400 ± 800 [−1.6]
8	ND	ND	ND

[a] The $\Delta\Delta G_b$ values were calculated from the equation $-RT \ln[(k_{cat}/K_M)_X/(k_{cat}/K_M)_1]$ where R is the gas constant and T is the absolute temperature. The errors shown were obtained from calculated fits (KaleidaGraph-Synergy Software) of the data to the Michaelis-Menton equation. The errors in the k_{cat}/K_M values were from the propagation of the fitted k_{cat} and K_M errors.[49] [b] The $\Delta\Delta G_s$ values were calculated from the equation $-RT \ln[(K_M)_X/(K_M)_1]$, $\Delta\Delta G^{\ddagger}$ values were calculated from the equation $-RT \ln[(k_{cat})_X/(k_{cat})_1]$, where X corresponds to a substrate to which 1 is being compared.

substrates is due to differences in the expression of binding energy along the catalytic reaction coordinate.

Experimental Section

General Methods and Reagents. Reactions requiring anhydrous conditions were carried out in flame-dried glassware under an atmosphere of argon. Anhydrous solvents were purchased from Aldrich. Chromatography solvents were purchased from Fisher Corp. and were used as received. Reagents were purchased either from Sigma or Aldrich and used as received unless noted otherwise. ¹H NMR and ¹³C NMR were recorded on a General Electric 300 MHz instrument. The NMR samples were prepared in 5-mm tubes, and the chemical shifts are reported in parts per million (δ) relative to the TMS standard for samples in CDCl₃ and the TSP (3-(trimethylsilyl)-1-propanesulfonic acid sodium salt) standard for samples in D₂O. Flash chromatography was performed with Merck silica gel 60 (230−400 mesh). Ion exchange chromatography was performed with Diethylaminoethyl (DEAE) Sephadex A-25 (anion exchange) and Dowex 50WX2-100 (cation exchange). The resins were washed and prepared according to manufacturers' recommendations.

Synthesis of n-Formylated Amino Acid Ester Substrates, 1−8. The racemic phenyl ester substrates were synthesized as described by Wade and Scanlan.[9] The synthesis of **5** is described by Guo et al. The L-enantiomer of the amino acid esters (**1**, **2**, and **4**) was used in the temperature-dependent studies. The synthesis of the enantiopure substrates is described by Wade and Scanlan.[14]

n-Formyl-((*S*)-methyl)-cysteine phenyl ester [3]: yield 0.65 g (80%) ¹H NMR (300 MHz, CDCl₃) δ 8.29 (s, 1H), 7.40 (t, *J* = 7.8 Hz, 2H), 7.27 (t, *J* = 7.2 Hz, 1H), 7.13 (d, *J* = 8.2 Hz, 2H), 6.64 (br d, *J* = 7.5 Hz, 1H), 5.16 (dd, *J* = 7.8, 4.5 Hz, 1H), 3.16 (d, *J* = 5.1 Hz, 2H), 2.21 (s, 3H); ¹³C NMR δ 160.8, 129.6, 126.4, 121.2, 50.6, 36.3, 16.4; MS (EI) 239.0(M⁺), 239.1, 194.1, 160.0, 146.0, 118.0, 101.0,

(23) For another example of context-dependent expression of binding energy see Narlikar, G.; Herschlag, D. *Biochemistry* **1998**, *37*, 9902−9911. In this study with a *Tetrahymena* group I RNA enzyme, the authors find that the inclusion or removal of a specific binding interaction gives rise to a uniform binding effect in the WT ribozyme and provides specific transition-state stabilization in the context of a mutant ribozyme. These results suggest that the optimization of a catalyst and the contributions that binding interactions may make to catalysis depend on the context (i.e., the starting point) and the amount of binding energy available from other interactions. In our study, the starting point is 17E8 and the substrate that 17E8 was designed to cleave is (**2**).

Figure 3. Free energy diagrams representing binding energy use and catalysis. (A) 17E8 catalyzed reaction with **1** (black) and **2** (grey) (B) 17E8 catalyzed reaction with **1** (black) and **4** & **7** (grey). Both IgG and S represent unbound antibody and substrate, respectively. (IgG−S) and (IgG−S)‡ represent the Michaelis and transition-state complexes, respectively.

94.0, 90.0, 77.0, 61.0. HRMS calcd for $C_{12}H_{15}N_1O_3S_1$: 239.0616. Found: 239.0616.

 n-Formyl-((S)-ethyl)-cysteine phenyl ester [4]: yield 0.75 g (90%); ^{1}H NMR (300 MHz, CDCl$_3$) δ 8.22 (s, 1H), 7.36 (t, $J = 7.5$ Hz, 2H), 2.23 (t, $J = 7.2$ Hz, 1H), 7.10 (d, $J = 7.8$ Hz, 2H), 6.56 (br s, 1H), 5.10 (dd, $J = 9.0, 4.8$ Hz, 1H), 3.12 (d, $J = 4.5$ Hz, 2H), 2.58 (dd, $J = 7.5, 6.9$ Hz, 2H), 1.52 (t, $J = 7.2$ Hz, 2H); ^{13}C NMR d 169.1, 160.8, 150.3, 129.6, 126.4, 121.2; MS (EI) 253.1(M$^+$), 208.1, 160.0, 132.0, 115.0, 104.1, 94.0, 87.0, 75.0, 65.0. HRMS Calcd for $C_{12}H_{15}N_1O_3S_1$: 253.0773. Found: 253.0774.

 n-Formyl-(O-methyl)-serine phenyl ester [6]: yield 0.73 g (88%) ^{1}H NMR (300 MHz, CDCl$_3$) δ 8.30 (s, 1H), 7.40 (t, $J = 7.5$ Hz, 2H), 7.26 (t, $J = 7.8, 7.5$ Hz, 1H), 7.10 (d, $J = 7.5$ Hz, 2H), 6.54 (br d, $J = 5.4$ Hz, 1H), 5.08 (dt, $J = 8.4, 2.7$ Hz, 1H), 4.05 (dd, $J = 9.3, 3.0$ Hz, 1H), 3.77 (dd, $J = 9.3, 3.0$ Hz, 1H), 3.44 (s, 3H); ^{13}C NMR δ 160.7, 129.5, 126.3, 121.3, 72.2, 59.7, 51.5; MS (EI) 224.0(MH$^+$), 224.1, 130.1, 102.1, 94.0, 85.0, 74.1, 65.0. HRMS Calcd for $C_{11}H_{14}N_1O_4$: 224.0923. Found: 224.0915.

 n-Formyl-(O-ethyl)-serine phenyl ester [7]: yield 0.54 g (60%); ^{1}H NMR (300 MHz, CDCl$_3$) δ 8.30 (s, 1H), 7.40 (t, $J = 7.8, 7.5$ Hz, 2H), 7.26 (t, $J = 6.9$ Hz, 1H), 7.10 (d, $J = 7.8$ Hz, 2H), 6.56 (br d, $J = 5.4$ Hz, 1H), 5.10 (dd, $J = 8.4, 3.0$ Hz, 1H), 4.08 (dd, $J = 9.3, 2.4$ Hz, 1H), 3.79 (dd, $J = 9.3, 2.4$ Hz, 1H), 1.52 (q, $J = 6.9$ Hz, 2H) 1.22 (t, $J = 6.9$ Hz, 3H); ^{13}C NMR δ 160.6, 129.5, 126.2, 121.3, 70.1, 67.1, 51.5, 15.0; MS (EI) 238.1(MH$^+$), 238.1, 144.0, 133.0, 116.0, 94.0, 82.9, 70.0, 60.0. HRMS Calcd for $C_{12}H_{15}N_1O_4$: 237.1001. Found: 237.0995.

 n-Formyl-(O-methyl)-homoserine phenyl ester [8]: yield 0.57 g (63%) ^{1}H NMR (300 MHz, CDCl$_3$) δ 8.26 (s, 1H), 7.39 (t, $J = 7.8$ Hz, 2H), 7.25 (t, $J = 7.2$ Hz, 1H), 7.10 (d, $J = 7.8$ Hz, 2H), 6.85 (br d, $J = 5.4$ Hz, 1H), 5.10 (dt, $J = 7.2, 5.4$ Hz, 1H), 3.58 (t, $J = 5.7$ 2H), 3.35 (s, 3H), (q, $J = 5.4$ Hz, 2H) 1.22 (t, $J = 6.9$ Hz, 3H); ^{13}C NMR δ 170.3, 160.8, 150.5, 129.4, 126.0, 121.2, 68.9, 58.9, 49.7, 15.0; MS (EI) 238.1(MH$^+$), 179.1, 158.0, 116.1, 94.0, 82.9, 70.0, 65.0, 56.0. HRMS Calcd for $C_{12}H_{16}N_1O_4$: 238.1079. Found: 238.1087.

 Synthesis of n-Formylated Phenyl Phosphonates (see Figure 6a, 6b, and text for phosphonates used). The phosphonates were prepared by the route similar to that described by Guo et al. The use of aldehydes with different side chains yielded the series.

 Phenyl [1-(1-N-Formylamino)alkyl]phosphonates. 2-((S)-ethyl)-ethyl (corresponding substrate is **4** in Figure 2): yield 0.20 g (44%); ^{1}H NMR (300 MHz, D$_2$O) δ 8.22 (s, 1H), 7.45 (t, $J = 8$ Hz, 2H), 7.23 (t, $J = 8.0$ Hz, 1H), 7.19 (d, $J = 9$ Hz, 2H), 4.44 (ddd, $J = 15.2, 12, 3.2$ Hz, 1H), 3.22 (ddd, $J = 14.4, 4.8, 3.2$ Hz, 1H), 2.80 (ddd, $J = 14.4, 12, 6$ Hz, 1H), 2.61 (dq, $J = 7.2, 2.4$ Hz, 2H), 1.20 (t, $J = 7.2$ Hz, 3H) LSIMS-MS(−) 288.4 m/z (MH$^-$−HCl).
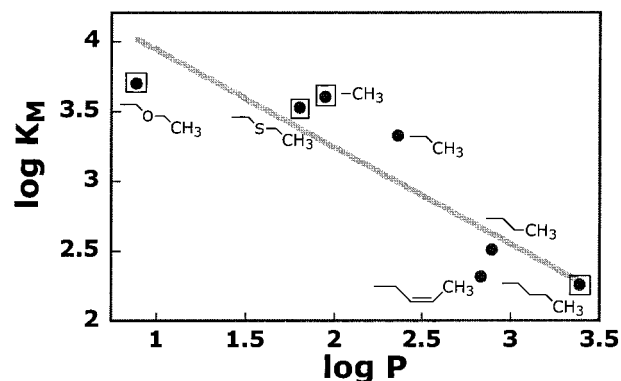
Figure 4. Correlation between log P and log K_M values of the substrates used in the 17E8 catalyzed reaction. The K_M values for the substrates that are not discussed in this paper were taken from ref 12. The concentration units for the substrates are μM. The log P values correspond to those of model compounds that are analogous to the side chains of the phenyl ester substrates: pentane, log $P = 3.39$, **2**; cis 3-pentene, 2.83; butane, 2.89; propane, 2.36; ethane, 1.81, **1**; diethyl sulfide, 1.95, **4**; diethyl ether, 0.89, **7**. The values were taken from ref 24. The boxed data designate the substrates that are discussed in this paper. The slope of the line without **4** and **7** is −0.9 ± 0.2, $R = 0.93$; with **4** and **7** included, the slope is −0.7 ± 0.2, $R = 0.90$.
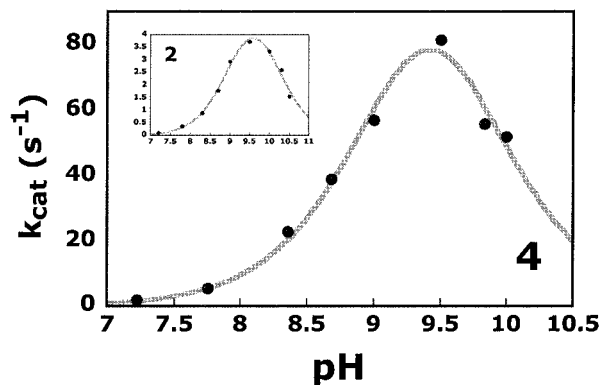

Figure 5. pH-k_{cat} profile for 17E8 catalyzed hydrolysis of **2** (inset) and **4**. The pK_a values obtained from the fit to the following equation:

$$k_{cat(obs)} = \frac{k_o}{10^{pK_{a1}-pH} + 1 + 10^{pH-pK_{a2'}}}$$

where $k_{cat(obs)}$ is the observed k_{cat} value and k_o is the pH independent k_{cat} value. The equation was derived from a scheme based on two ionizable antibody residues (for a model see ref 27). The pK_{a1} and pK_{a2} values obtained for the substrates are 9.2 ± 0.2 and 9.7 ± 0.2, $R = 0.993$ (**4**), and 9.0 ± 0.1 and 10.0 ± 0.1, $R = 0.994$ (**2**).

 3-(S-methyl)-propyl (corresponding substrate is **5**) (44%): ^{1}H NMR (300 MHz, D$_2$O) δ 8.16 (s, 1H), 7.41 (t, $J = 6.8$ Hz, 2H), 7.22 (t, $J = 7.6$ Hz, 1H), 7.17 (d, $J = 8.4$ Hz, 2H), 4.45 (ddd, $J = 14.8, 11.2, 3.2$ Hz, 1H), 2.69 (ddd, $J = 13.6, 8.4, 4.8$ Hz, 1H), 2.80 (dt, $J = 13.2, 8.4$ Hz, 1H), 2.17 (m, 1H), 2.11 (s, 3H), 1.96 (s, 1H) LSIMS-MS(−) 288.4 m/z (MH$^-$−HCl).

 Steady-State Kinetics of the Phenyl Esters. Michaelis-Menton parameters for the substrates were determined by continuous measurement at 270 nm (phenol release $\epsilon = 1400$ M^{-1}·cm^{-1}) using a Uvikon 930 (Kontron Instrument) UV−vis spectrophotometer. All assays were performed with cuvette holders thermostated at 24.5 ± 0.5 °C with a Lauda RM6 temperature control unit. Cells of 1-cm path length (0.5 mL) were used in each experiment. The buffer used in all kinetic experiments was 50 mM borate−150 mM NaCl, pH 8.7. The antibody concentrations used in the experiments ranged from 0.2 to 1.4 μM. All substrates were soluble at these substrate concentrations. The substrate concentrations used were: **1**, 800 μM to 30 mM; **2**, 30 μM to 1 mM; **3**, 650 μM to 22 mM; **4**, 200 μM to 25 mM. The reactions were initiated by adding 20 mL of the substrate stock in DMSO to a solution of 13−
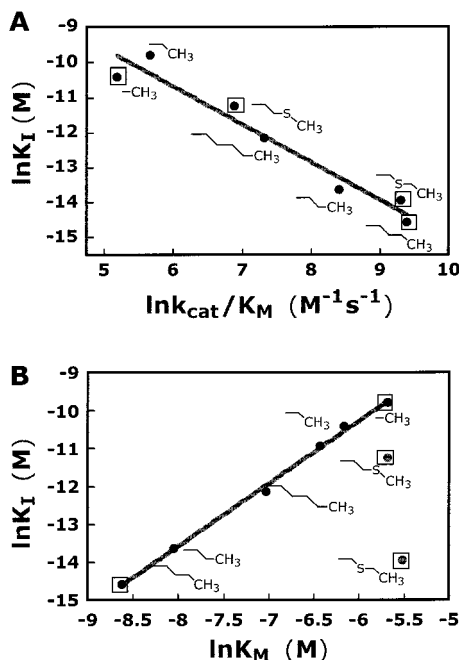
Figure 6. Transition-state versus substrate complementarity. (A) ln K_I vs ln k_{cat}/K_M (slope $= -1.08 \pm 0.11$ $R = 0.973$). (B) ln K_I vs ln K_M (slope $= 1.64 \pm 0.05$ $R = 0.999$). The data used in the plots were obtained using various phenyl ester substrates and phosphonates. The substrate and phosphonate skeletons are shown in Figure 2. The side chains are shown next to the data points. The data were fit with the KaleidaGraph curve-fitting program (data taken from refs 9 and 14 and Table 1). The boxed data designate the substrates that are discussed in this paper.

25 mL of 17E8 (in PBS) and 455−467 mL of pH 8.7 borate buffer. In the background reactions, the IgG was replaced with PBS. All catalyzed assays were performed in triplicate. The background reactions were performed in duplicate. The catalyzed rate was obtained by subtracting the average of the background reaction rate from the rate of the catalyzed reaction. The data (v vs [S]) from the experiments were fit with the KaleidaGraph (Synergy Software) curve-fitting program using the Michaelis-Menten equation.

pH-Rate Dependence of 17E8 Catalysis. The steady-state kinetic parameters of 17E8 catalysis of **4** at different pH values were obtained in the same manner as described above for the experiments performed at pH 8.7. The following buffer systems were used in this analysis: 50 mM $NaHPO_4$, 150 mM NaCl, pH 7.2; 50 mM Tris, 150 mM NaCl, pH 7.8; 50 mM borate, 150 mM NaCl, pH 8.4, pH 8.7; 50 mM CHES, 150 mM NaCl, pH 9.0, pH 9.5, pH 9.8, and pH 10.0. The buffer system used for **2** is listed in ref 27. The parameters for the pH values >10 were not obtained due to a high background reaction. The k_{cat} values were plotted as a function of pH to the equation described in the legend of Figure 5 using the KaleidaGraph plotting program.

Temperature Dependence of Catalysis. All reactions were performed in 50 mM borate, 150 mM NaCl (pH 8.0). The steady-state kinetic parameters of 17E8 catalysis of **1**, **2**, and **4** at the different temperatures were obtained in the same manner as described above for the experiments performed at 24.5 °C. The temperature range covered for each of the substrates was from 5 to 40 °C. The k_{cat}, K_M, and k_{cat}/K_M values for the different temperatures were plotted as a function of $1/T$ (K) to the equation described in the legend of Figure 7 using the KaleidaGraph plotting program.

Results and Discussion

To make 17E8 behave in a more catalytically optimized manner than that demonstrated with the substrates **1** and **2**, we attempted to circumvent the uniform use of the side-chain−pocket binding energy by destabilizing the (IgG−S). This destabilization would leave some of the binding energy to be
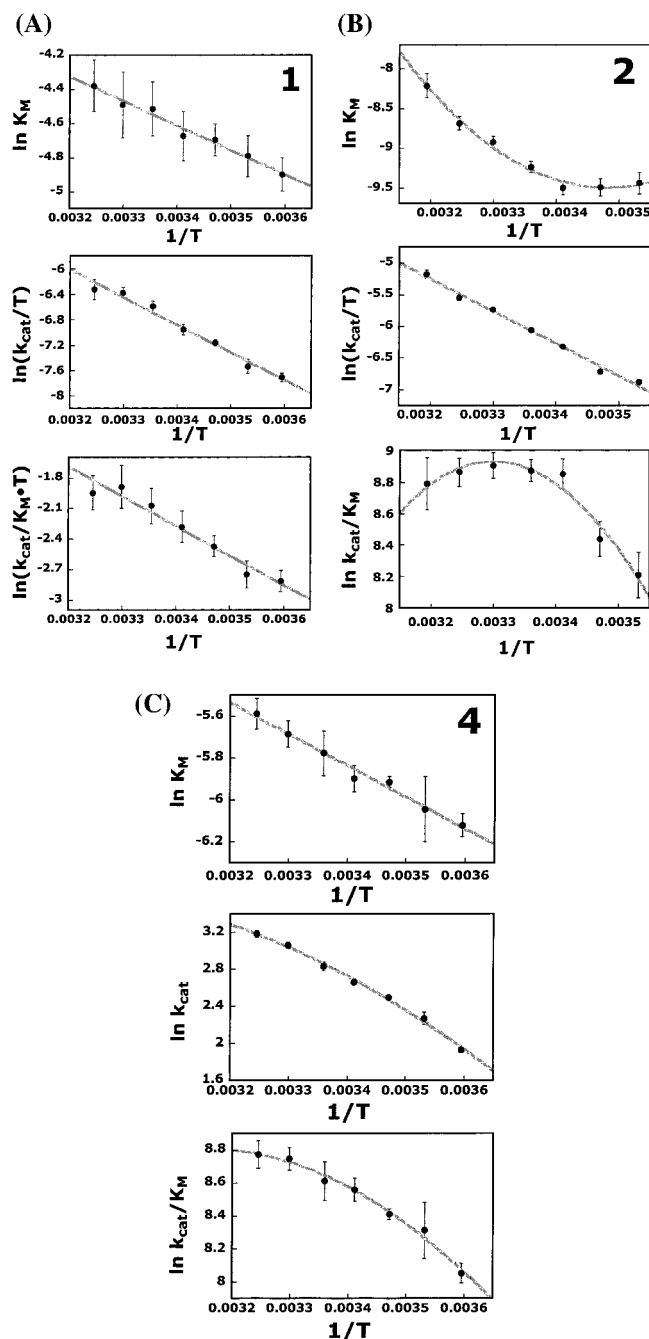
Figure 7. Temperature dependence of K_M, k_{cat}, and k_{cat}/K_M for **1** (A), **2** (B), and **4** (C). The K_M data for **1** and **4** were fit to the equation: ln $K_M = (\Delta H^o/RT) - (\Delta S^o/R)$. *The K_M data for **2** was fit to the equation* ln $K_M = (\Delta H^o_{T(0)}/RT) - ((\Delta S^\ddagger_{T(0)} - \Delta Cp^o)/R) - (\Delta Cp^o \ln T/R)$, where $\Delta H^o_{T(0)}$ and $\Delta S^o_{T(0)}$ are the enthalpy and entropy change at 0 K. The k_{cat} data for **1** and **2** were fit to the equation: $\ln(k_{cat}/T) = \ln(k_b/h) + (\Delta S^\ddagger/R) - (\Delta H^\ddagger/RT)$. The k_{cat} data for **4** was fit to the equation ln $k_{cat} = \ln(k_b/h) - (\Delta H^\ddagger_{T(0)}/RT) + (1 + (\Delta Cp^\ddagger/R)) \ln T + ((\Delta S^\ddagger_{T(0)} - \Delta Cp^\ddagger)/R)$, where $\Delta H^\ddagger_{T(0)}$ and $\Delta S^\ddagger_{T(0)}$ are the enthalpy and entropy of activation at 0 K, respectively. The k_{cat}/K_M data for **1** was fit to the equation: $\ln(k_{cat}/K_M T) = \ln(k_b/h) + (\Delta S^\ddagger/R) - (\Delta H^\ddagger/RT)$. The k_{cat}/K_M data for **2** and **4** were fit to the equation: $\ln(k_{cat}/K_M) = \ln(k_b/h) - (\Delta H^\ddagger_{T(0)}/RT) + (1 + (\Delta Cp^\ddagger/R)) \ln T + ((\Delta S^\ddagger_{T(0)} - \Delta Cp^\ddagger)/R)$.

used to decrease the free-energy difference between the (IgG−S) and the (IgG−S)‡ and increase k_{cat}. We decided to exploit the correlation between the stability of the (IgG−S), log K_M, and the hydrophobicity parameter, log P, for the substrate side chains (Figure 4). The relationship suggests that the Michaelis complex can be destabilized by using substrates with side chains

that are less hydrophobic than **2**. There is also a modest correlation between $\log(k_{cat}/K_M)$ and $\log P$.[9] It is unclear if either correlation is due to the removal of side-chain−pocket contacts or to side-chain hydrophobicity. Unfortunately, these factors are inextricably linked, so we decided to change the hydrophobicity of the side chain while maintaining the maximum number of heavy-atom−pocket contacts to reduce destabilization of the (IgG−S)‡ complex. By replacing methylene groups in the side chain with sulfur and oxygen atoms, the hydrophobicity of the side chain is substantially altered as indicated by the changes in the $\log P$ values (Figure 4) which are directly correlated to the free energy of transfer from octanol to water for model compounds.[24]

The steady-state kinetic parameters for the substrates are shown in Table 1. As predicted by the $\log P$−$\log K_M$ correlation for the homologous aliphatic side-chain series, the heteroatom replacement results in destabilization of the (IgG−S) as indicated by the large increases in K_M and the unfavorable $\Delta\Delta G_s$ values which are as large as 2 kcal/mol (relative to **2**). The K_M values for the substrates with the oxygen replacements (**6**−**8**) are larger than those for those with the sulfur replacements (**3**−**5**) further substantiating the $\log P$−$\log K_M$ trend. The inclusion of these substrates on the $\log K_M$−$\log P$ plot maintains the linear relationship between the two parameters (Figure 4). The heteroatom replacements do not result in significant changes in the k_{cat}/K_M values (compare **4**, **5**, and **7** to **1**) which is in contrast to the result of deleting methylene groups (compare **1** and **2**). The heteroatom replacements do result in increased k_{cat} values for the 17E8 catalyzed reactions. The k_{cat} increase is as high as 20-fold (**8**) and is dependent on the heteroatom position in the side chain. The γ-replacements (**3**, **4** and **6**, **7**) had much larger increases than the δ-replacements (**5** & **8**).

The kinetic behavior of these alternative substrates suggests that the side-chain−pocket binding energy is being used *differentially* between the (IgG−S) and the (IgG−S)‡ (see Figure 3).[1,2,4] When the additional binding groups are added to **1** to yield **3**−**7**, the (IgG−S) complex is not further stabilized, in contrast to the **1** to **2** side-chain change. However, the additional groups do significantly stabilize the (IgG−S)‡ complex as shown by the negative $\Delta\Delta G_b$ values that are more favorable by as much as 2 kcal/mol. These increases in k_{cat} values for substrates **3**−**7** suggest that the additional interactions are used to decrease the free-energy difference between the (IgG−S) and (IgG−S)‡ complexes. The $\Delta\Delta G^{\ddagger}$ value (relative to **1**) is decreased by as much as 1.7 kcal/mol.

To ensure that the changes in the kinetic parameters were due to differential binding and not to a change in the catalytic mechanism, we performed a pH-rate study for substrate **4**, which is the substrate that has the highest increase in turnover number (Figure 5). The shape of the plot and the two pK_a values obtained for **4** are similar to those for **2**, suggesting that the same residues participate in the rate-determining step for the catalyzed hydrolysis of **2** and **4**.[25−27]

The phosphonate transition-state analogue corresponding to substrate **4** was also synthesized and tested for its binding and inhibition activity related to the 17E8 catalyzed reaction (see Figure 2 for structure). The phosphonate is a competitive

inhibitor of the 17E8 reaction and has an inhibition and binding constant similar to that of the phosphonate corresponding to **2** (data not shown). The $\ln K_I$ and $\ln(k_{cat}/K_M)$ relationship for the substrates and their corresponding transition-state analogues is also maintained with the inclusion of substrates **3** and **4**, supporting the similarity in transition-state structure for **2**, **3**, and **4** hydrolysis (Figure 6).[28−31] These results support the kinetic evidence that points to differential binding as the cause for the increase in turnover rate. The tight binding of the transition-state analogue also discounts the possibility that the increase in turnover rate is solely due to an increase in the intrinsic reactivity of the ester with the replacement of the heteroatom.[32]

To obtain further insight into the mechanistic differences in the catalyzed hydrolysis of substrates **1**, **2**, and **4**, the temperature dependence of 17E8 catalysis with each of the substrates was studied. The temperature dependence of the steady-state parameters K_M, k_{cat}, and k_{cat}/K_M yielded the thermodynamic quantities shown in Table 2.[33] The ΔH_{KM} values obtained for substrate binding are −7.0, −2.9, and −2.8 kcal/mol for **1**, **2**, and **4**, respectively. The ΔS_{KM} values are 6.3, 1.4, −0.5 cal/(mol·K).[34] The van't Hoff plot for substrate **2** results in a curved data fit which suggests that the ΔH_{KM} and ΔS_{KM} values are not constant with temperature and that a ΔCp_{KM} must be included in the van't Hoff equation (Figure 7B).[35] The ΔCp_{KM} value obtained from the fit is 700 cal/(mol·K).[36] There is no observed curvature in the $\ln K_M$−$1/T$ plot with substrates **1** and **4** (Figure 7A,C).[37] The data for the k_{cat} dependence on temperature yields $\Delta H^{\ddagger}_{kcat}$ values of 10.1, 5.6, and 8.6 kcal/mol and $\Delta S^{\ddagger}_{kcat}$ values of −32, −25, and −32 cal/(mol·K) for **1**, **2**, and **4**, respectively. The plot of $\ln(k_{cat}/T)$ vs $1/T$ for **4** suggests that $\Delta H^{\ddagger}_{kcat}$ and $\Delta S^{\ddagger}_{kcat}$ values are not constant with temperature for the reaction with **4** (Figure 7C).[38] The $\Delta Cp^{\ddagger}_{kcat}$ value obtained from the fit is 140 cal/(mol·K). No curvature is seen in the $\ln(k_{cat}/T)$ vs $1/T$ plots for **1** and **2** (Figure 7A,B). The k_{cat}/K_M temperature dependence data yields $\Delta H^{\ddagger}_{TS}$ values of 2.6, 2.5, and 5.8 kcal/

(28) Mader, M. M.; Bartlett, P. A. *Chem. Rev.* **1997**, *97*, 1281−1301.

(29) Bartlett, P. A.; Marlowe, C. K. *Biochemistry* **1983**, *22*, 4618−4624.

(30) Wolfenden, R. *Annu. Rev. Biophys. Bioeng.* **1976**, *5*, 271−306.

(31) Gandour, R. D.; Schowen, R. L. *Transition States of Biochemical Processes*; Plenum Press: New York, 1978.

(32) The larger k_{cat} value for **4** (compared with that of **7**) also suggests that an increase in the intrinsic reactivity of the carbonyl due to the heteroatom replacement is not a large factor as the oxygen replacement should render the carbonyl group more reactive than the sulfur atom replacement.

(33) It should be pointed out that because there is a pH rate dependence for the catalyzed reaction, it is therefore possible that the parameters obtained from the temperature dependence ($\Delta H^{\ddagger}$, ΔH_{KM}, $\Delta S^{\ddagger}$, and ΔS_{KM}) include contributions from the protonation and deprotonation of active-site residues. For the study presented, we emphasize the *differences* in the parameters obtained for the substrates. The contributions from the protonation and deprotonation of the active-site residues are most likely the same for the substrates, as they are cleaved by the same mechanism, with the participation of the same active-site residues, and have similar transition-state structures.

(34) Although the ΔS_{KM} may seem anomalous for a binding event, similar values have been noted for binding of substrates in other enzymatic systems. Hinz, H.; Weber, K.; Flossdorf, J.; Kula, M. *Eur. J. Biochem.* **1976**, *71*, 437−442; Sturtevant, J. M. *Proc. Natl. Acad. Sci. U.S.A.* **1977**, *74*, 2236−2240; Fukuda, M.; Kunugi, S. *Eur. J. Biochem.* **1984**, *71*, 565−570; and Ross, P. D.; Subramanian, S. *Biochemistry* **1981**, *20*, 3096−3102. These positive and near-zero values for the association of the substrate with 17E8 are consistent with the release of bound water for the 17E8 active site and from the substrate's hydrophobic moieties (phenyl group and side chain).

(35) In this study, we assume that K_M is approximately equal to K_S. We believe this assumption to be reasonable for several reasons. The turnover rate for 17E8 is not fast enough to warrant the suggestion that $k_{off} > k_{cat}$, thus leaving term K_M devoid of chemical steps. The existence of additional unimolecular nonchemical steps (i.e., protein conformational change) which would precede the rate-determining chemical step is unlikely, due to the simple catalytic mechanisms elicited by phosphonate haptens. The rate-determining nature of the hydrolysis of the phenyl ester has been determined in other mechanistic studies (see ref 27).
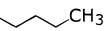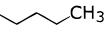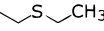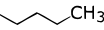
(24) Hansch, C.; Leo, A.; Hoekman, D. *Exploring QSAR: Hydrophobic, Electronic, and Steric Constants*; American Chemical Society: Washington, D. C., 1995.

(25) Zhou, G. W.; Guo, J.; Huang, W.; Fletterick, R. J.; Scanlan, T. S. *Science (Washington, D.C.)* **1994**, *265*, 1059−1064.

(26) Guo, J.; Huang, W.; Zhou, W.; Fletterick, R. J.; Scanlan, T. S. *Proc. Natl. Acad. Sci. U.S.A.* **1995**, *92*, 1694−1698.

(27) Guo, J.; Huang, W.; Scanlan, T. S. *J. Am. Chem. Soc.* **1994**, *116*, 6062−6069.

Table 2. The Thermodynamic Quantities Obtained from the Temperature Dependence of k_{Cat}, K_M, and k_{Cat}/K_M[a]

| | $1/K_M$[a] | | |
substrate	ΔH_{KM}[b] kcal/mol	ΔS_{KM} cal/(mol·K)	$\Delta C p_{KM}$ cal/(mol·K)
[1] $-CH_3$	-2.8 ± 0.2	0.5 ± 0.6	
[2] $\diagup\!\!\diagdown\!\!\diagup CH_3$	-7.0 ± 0.9	6.4 ± 0.7	700 ± 80
[3] $\diagdown\!\!S\!\!\diagup CH_3$	-2.9 ± 0.2	-1.4 ± 0.6	
	k_{cat}		
substrate	$\Delta H^{\ddagger}_{kcat}$[c] kcal/mol	$\Delta S^{\ddagger}_{kcat}$ cal/(mol·K)	$\Delta C p^{\ddagger}_{kcat}$ cal/(mol·K)
[1] $-CH_3$	8.6 ± 0.5	-32 ± 2	
[2] $\diagup\!\!\diagdown\!\!\diagup CH_3$	10.1 ± 0.4	-26 ± 1	
[3] $\diagdown\!\!S\!\!\diagup CH_3$	5.6 ± 0.7	-34 ± 5	-140 ± 50
	k_{cat}/K_M		
substrate	$\Delta H^{\ddagger}_{TS}$ kcal/mol	$\Delta S^{\ddagger}_{TS}$ cal/(mol·K)	$\Delta C p^{\ddagger}_{TS}$ cal/(mol·K)
[1] $-CH_3$	5.8 ± 0.6	-32 ± 2	
[2] $\diagup\!\!\diagdown\!\!\diagup CH_3$	2.0 ± 0.3	-32 ± 1	-620 ± 110
[3] $\diagdown\!\!S\!\!\diagup CH_3$	2.1 ± 0.5	-33 ± 4	-170 ± 50

[a] The values of $1/K_M$ are shown so that the values represent those for formation of the Michaelis complex as K_M formally represents a dissociation constant. [b] The ΔH_{KM} and ΔS_{KM} values at 298 K for **2** were calculated from the fits in Figure 7 using the equations:

$$\Delta H^o_{298K} = \Delta H^o_{T(0)} + T\Delta Cp^o \text{ and } \Delta S^o_{298K} = \Delta S^o_{T(0)} + \Delta Cp^o \ln T$$

[c] The $\Delta H^{\ddagger}_{kcat}$ and $\Delta S^{\ddagger}_{kcat}$ values at 298 K for 2 were calculated from the fits in Figure 7 using the equations:

$$\Delta H^{\ddagger}_{298K} = \Delta H^{\ddagger}_{T(0)} + T\Delta Cp^{\ddagger} \text{ and } \Delta S^{\ddagger}_{298K} = \Delta S^{\ddagger}_{T(0)} + \Delta Cp^{\ddagger} \ln T$$

mol and $\Delta S^{\ddagger}_{TS}$ values of -32, -33, and -32 cal/(mol·K) for **1**, **2**, and **4**, respectively. The curved $\ln(k_{cat}/K_M)$ vs $1/T$ plot yields $\Delta Cp^{\ddagger}_{TS}$ values of 620 and 170 cal/(mol·K) for **2** and **4**, respectively.

(36) We believe this ΔCp value to be an overestimate. One reason is the inherent difficulty in obtaining accurate heat-capacity changes from van't Hoff plots. Another reason it that the heat capacity of binding of the phosphonates that correspond to **1**, **2**, and **4** obtained by calorimetric experiments are much smaller (>2-fold) than the ΔCP_{KM} and $\Delta Cp^{\ddagger}$ obtained by the temperature dependence of the kinetic constants. The heat capacity changes for phosphonate binding are probably underestimates as charged moieties contribute to heat capacity with opposite magnitude as do hydrophobic moieties. The fit obtained from Figure 8 is not very sensitive to the ΔCp variable. Changing the ΔCp from 700 to 300 cal/(mol·K) had a very small change on ΔH_{KM} (7.0 and 6.8 kcal/mol) and ΔS_{KM} (-6.4 and -6.6 cal/(mol·K)), respectively. The correlation coefficients are 0.995 and 0.971, respectively.

(37) The curvature of the $\ln K_M - 1/T$ plot could also arise because of a shift in equilibrium between several (17E8−substrate) complexes or the involvement of chemical rate constants in the Michaelis constant. The involvement of several Michaelis complex forms seems unlikely due to the absence of curvature seen in the $\ln K_M - 1/T$ plots with substrates **1** and **4**. If there was an obligatory isomerization of the Michaelis complex for 17E8 catalysis, one would expect to see the same with other substrates that are processed by the catalyst. The linear nature of the $\ln(k_{cat}/T) - 1/T$ plot is also consistent with the nonexistence of several Michaelis-like complexes. The "well-behaved" nature of the plot also suggests that there is no equilibrium shift in the ground state for 17E8 catalysis.

(38) The data also can be fitted to the standard Eyring equation (no $\Delta Cp^{\ddagger}$ included). This yields $\Delta H^{\ddagger}$ and $\Delta S^{\ddagger}$ values of 6.3 kcal/mol and -32 cal/(mol·K), respectively. The R value for the fit to the standard equation is 0.993. The R value for the fit that includes a $\Delta Cp^{\ddagger}$ contribution is 0.998.

From these thermodynamic quantities, a model of the use of side-chain−pocket interactions along 17E8's hydrolytic reaction coordinate can be postulated. The more favorable ΔH_{KM} for **2** suggests that more interactions are formed in the (**2**−17E8) complex than in the (S−17E8) complexes with **1** and **4**. The $\Delta\Delta H_{KM}$ of binding between **1** and **3** is essentially zero, suggesting that a similar number of interactions are formed in the (**1**−17E8) and (**4**−17E8) complexes. The large ΔCp_{KM} value suggests that the interactions formed in the (**2**−17E8) complex are hydrophobic in nature which is expected due to the structure of the *n*-butyl moiety and the residues that surround the side-chain in the transition-state−17E8 complex.[39−43] The lack of an observable ΔCp_{KM} and the enthalpic similarity between (**1**−17E8) and (**4**−17E8) suggests that the side chain does not make substantial contact with the recognition pocket in the Michaelis complex of 17E8 and **4**.

The $\Delta H^{\ddagger}_{kcat}$ is most favorable for **4**, suggesting that more binding interactions are used in the transformation of (IgG−**4**) to (IgG−**4**)‡ than with **1** and **2**. The curvature in the $\ln(k_{cat}/T)−1/T$ plot suggests that the hydrophobic effect is playing a role in the turnover of the (IgG−**4**) complex. The $\Delta Cp^{\ddagger}$ (**4**) value is smaller than the ΔCp_{KM} (**1**) value. This is expected as the group contribution of −S− to ΔCp is smaller than that of a −CH$_2$− group.[42,44] The large negative $\Delta S^{\ddagger}_{kcat}$ for the substrates suggests that the transition-state complexes are substantially more ordered than the substrates' respective Michaelis complexes. This can be explained by the fact that more contacts are made in the transition-state complex (especially with the oxyanion hole) and the fact that a water molecule must become fixed to participate in the transition state of the reaction.

The postulated models for 17E8's use of the side-chain−pocket interactions are shown in Figure 8. The side-chain contacts are used extensively with **2** in the Michaelis complex and much less so with **4** as suggest by the ΔH_{KM} values and the ΔCp_{KM} for **2**. The side-chain contacts are used in converting the (IgG−**4**) complex to its transition-state complex as suggested by the $\Delta H^{\ddagger}_{kcat}$ and $\Delta Cp^{\ddagger}_{kcat}$ values. Substrate **1** cannot make many contacts in either complex and thus has been used as a control substrate to determine if the curvature in the temperature-dependent plots indeed results from the extended side-chain−pocket contacts. The similar $\Delta H^{\ddagger}_{TS}$ and $\Delta S^{\ddagger}_{TS}$ values for **2** and **4** suggest that their transition-state complexes are highly similar. Thus, it seems that the side chains for **2** and **4** are being used differently in the 17E8-catalyzed reactions.

One reason that enzymes are able to achieve differential binding of specific groups on substrates is because their active sites are often more complementary to the transition state than to the Michaelis complex.[2,4,28,31,45] The existence of a linear correlation between $\ln(k_{cat}/K_M)$ and $\ln K_I$, a lack of a correlation between $\ln K_M$ and $\ln K_I$ for alternative substrates, and transition-state analogues with several enzymes is proof of this comple-

(39) Ross, P. D.; Subramanian, S. *Biochemistry* **1981**, *20*, 3096−3102.

(40) Baldwin, R. L. *Proc. Natl. Acad. Sci. U.S.A.* **1986**, *83*, 8069−8072.

(41) Sturtevant, J. M. *Proc. Natl. Acad. Sci. U.S.A.* **1977**, *74*, 2236−2240.

(42) Edsall, J. T. *J. Am. Chem. Soc.* **1935**, *57*, 1506−1507.

(43) In addition to the hydrophobic effect, it has been noted that the existence of a heat capacity change may also result from contributions from intramolecular vibrations, electrostatic charges, hydrogen bonds, conformational entropy, and possibly changes in equilibria. The contribution electrostatic charges and hydrogen bonds is thought to be small due to the small net change in electrostatic interactions and hydrogen bonds upon binding. No correction has been made for conformational entropy and internal vibrational contributions to the heat-capacity change. The likelihood of possible changes in equilibria has been discussed (see footnote 37 and ref 41).

(44) Creighton, T. E. *Proteins: Structure and Molecular Properties*, 2nd ed.; W. H. Freeman and Company: New York, 1993.
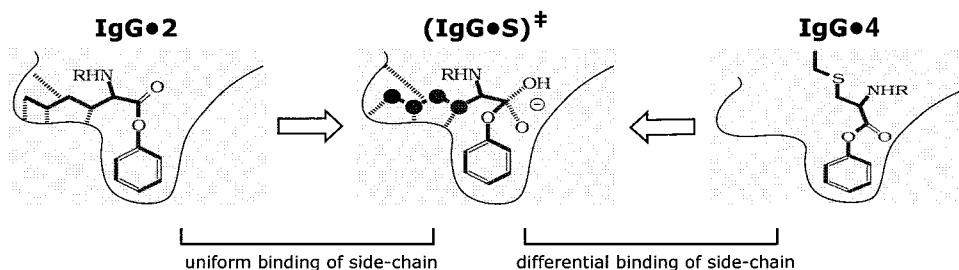
Figure 8. Postulated model of the side-chain−pocket interactions that result in uniform binding (substrate **2**) and differential binding (substrate **4**). In uniform binding, all the side-chain−pocket interactions are made in the (IgG−S) complex and no additional interactions are formed in the (IgG−S)‡. In differential binding, the side-chain−pocket interactions are formed exclusively in the (IgG−S)‡.

mentarity.[28,29,46−49] We have shown in our system that the ln-(k_{cat}/K_M) values of an extensive panel of substrates correlates well with the binding of the corresponding phosphonates, indicating that the side-chain−pocket interactions are similarly presented by both the catalytic transition state and the phosphonates.[9] The correlation between $\ln K_M$ and $\ln K_I$ in Figure 6 indicates that the side-chain−pocket interactions are similar in the Michaelis complex and in the transition state. This correlation suggests that part of 17E8's active site is complementary to both the ground state and the transition state. This precludes the possibility that the side-chain−pocket can be used differentially between the two species. The substrates **3** and **4** deviate from the $K_M−K_I$ correlation which is consistent with the side chains binding differently in the ground and the transition states.

In addition to engineering catalytic efficiency in the form of high k_{cat}/K_M values, an important concern in catalyst design is high turnover (large k_{cat} values). The properties of enzymes indicate that high turnover can be obtained by binding nonreactive portions of the substrate differentially between the ground- and transition-state complexes. This points out a potentially

significant limitation of generating catalytic antibodies with hapten molecules designed to mimic a transition state. There may often be a subtle structural difference between the transition state and the Michaelis complex for a chemical reaction that is not effectively exploited with a synthetic transition-state mimic. As a result, the antibodies generated against the transition-state analogue also bind corresponding nonreactive portions of the substrate with high affinity. Thus, haptens programs binding interactions needed to stabilize the transition state, but do not enforce the differential use of binding energy of nonreactive portions of the substrate. This inevitably results in the unproductive stabilization of antibody-bound ground state species. Thus, the development of new general strategies that can program or select for differential binding is undoubtedly an essential step for achieving truly efficient catalytic antibodies.

(45) Wolfenden, R. *Molecular and Cellular Biochemistry* **1974**, *3*, 207−211.

(46) Bartlett, P.; Otake, A. *J. Org. Chem.* **1995**, *60*, 3107−3111.

(47) Bartlett, P. A.; Giangiordano, M. A. *J. Org. Chem.* **1996**, *61*, 3433−3438.

(48) Phillips, M. A.; Kaplan, A. P.; Rutter, W. J.; Bartlett, P. A. *Biochemistry* **1992**, *31*, 959−963.

(49) Bevington, P. R.; Robinson, D. K. *Data Reduction and Error Analysis for the Physical Sciences*; 2nd ed.; McGraw-Hill: New York, 1992; p 328.